Time-Resolved Spectroscopic Measurements of Shock-Wave Induced Decomposition in Cyclotrimethylene Trinitramine (RDX) Crystals: Anisotropic Response

ARTICLE *in* THE JOURNAL OF PHYSICAL CHEMISTRY A · OCTOBER 2010

Impact Factor: 2.69 · DOI: 10.1021/jp106892c · Source: PubMed

Time-Resolved Spectroscopic Measurements of Shock-Wave Induced Decomposition in Cyclotrimethylene Trinitramine (RDX) Crystals: Anisotropic Response

Nhan C. Dang,[†] Zbigniew A. Dreger,*[,†] Yogendra M. Gupta,[†] and Daniel E. Hooks[‡]

Institute for Shock Physics and Department of Physics, Washington State University, Pullman, Washington 99164-2816, United States, and Dynamic & Energetic Materials Division, Los Alamos National Laboratory, Los Alamos, New Mexico 87545, United States

Received: July 23, 2010; Revised Manuscript Received: September 21, 2010

Plate impact experiments on the (210), (100), and (111) planes were performed to examine the role of crystalline anisotropy on the shock-induced decomposition of cyclotrimethylenetrinitramine (RDX) crystals. Time-resolved emission spectroscopy was used to probe the decomposition of single crystals shocked to peak stresses ranging between 7 and 20 GPa. Emission produced by decomposition intermediates was analyzed in terms of induction time to emission, emission intensity, and the emission spectra shapes as a function of stress and time. Utilizing these features, we found that the shock-induced decomposition of RDX crystals exhibits considerable anisotropy. Crystals shocked on the (210) and (100) planes were more sensitive to decomposition than crystals shocked on the (111) plane. The possible sources of the observed anisotropy are discussed with regard to the inelastic deformation mechanisms of shocked RDX. Our results suggest that, despite the anisotropy observed for shock initiation, decomposition pathways for all three orientations are similar.

1. Introduction

Understanding the role of crystal anisotropy on the shock wave initiation of high explosive (HE) crystals is fundamental to developing a basic understanding of HE sensitivity. The importance of crystalline anisotropy to the shock sensitivity of HE crystals was pointed out by Dick in his work on pentaerythritol tetranitrate (PETN).[1] He found that under plane shock wave compression, the time and run distance to detonation in PETN crystals depended strongly on the direction of shock wave propagation relative to the crystal axes.

Further work by Dick and co-workers[2−4] related the observed anisotropy in PETN sensitivity to the anisotropy in its Hugoniot elastic limit. This dynamic yield correlated with the anisotropic activation of known slip systems under shock wave compression. By extension, higher sensitivity was associated with steric hindrance, or the resistance to molecular motion, across slip interfaces. Recently, Winey and Gupta[5] described a continuum, anisotropic, thermomechanical model for PETN single crystals. Simulations employing this model reproduced the observed anisotropic wave profiles of the earlier experimental work.[3]

Using quantum calculations and optical spectroscopy measurements under shock compression and under static compression, Gupta and co-workers[6−9] have associated the mechanical deformation studies cited above to conformational changes in PETN molecules across slip planes. The conformational changes, which enable more facile subsequent reactivity, were consistent with the observed anisotropy in sensitivity to chemical decomposition. Based upon this mechanism, a molecular model for decomposition in shocked PETN, consistent with the experimental findings, was proposed.[7]

The above cited studies[1−9] on PETN crystals provided a molecular-to-continuum interpretation of anisotropic sensitivity under shock compression. However, it is not clear whether HE crystals, in general, display the anisotropic sensitivity and related phenomena observed in shocked PETN crystals. To address this question, we examined the anisotropic response of shocked cyclotrimethylene trinitramine (RDX), an important HE crystal used extensively in explosive formulations.

Because RDX is more resistant to shock initiation than PETN, studies of RDX anisotropy have focused mainly on the low stress regime below the reaction threshold.[10] Continuum wave profile measurements at stresses of 2.25 GPa revealed anisotropic mechanical response for shocked RDX single crystals.[10] Further, lower stress experiments (1.25 GPa) on (111) oriented crystals indicated that the qualitative features of the wave profiles depend on the input shock stress. Molecular dynamics (MD) simulations suggested that the observed stress-dependent changes in elastic-plastic response for (111) oriented RDX are caused by homogeneous nucleation of partial dislocations under shock-wave loading.[11] Moreover, spectroscopic studies up to 5.5 GPa showed no measurable orientation dependence either in the Raman shifts or in the shock induced $\alpha-\gamma$ phase transition that occurs at ~4.5 GPa.[12−14] All these studies suggests that below the decomposition threshold, the anisotropic response of RDX cannot be simply predicted from the slip systems determined under quasistatic loading.

Here, we extend our previous spectroscopic studies to examine the anisotropic response of RDX crystals to shock compression above the decomposition threshold. As in previous work,[10,13−15] plate impact experiments were performed on the (111), (210), and (100) planes to access 6, 5, and 0 different slip systems, respectively. The slip systems were determined in previous quasistatic loading studies.[16,17] In the orthorhombic space group, *Pbca*,[18] the available slip systems for (210) shocks were (021)[100], $(0\bar{2}1)$[100], (010)[100], (011)[100], and $(0\bar{1}1)$[100]. The same slip systems are available for (111) shocks, with the addition of the (010)[001] system.

Our previous work[15] demonstrated that shock-induced emission from (111) oriented RDX crystals can be attributed to the luminescence from species produced during RDX decomposition

* Corresponding author. E-mail: dreger@wsu.edu.
[†] Washington State University.
[‡] Los Alamos National Laboratory.

10.1021/jp106892c
Published on Web 10/08/2010

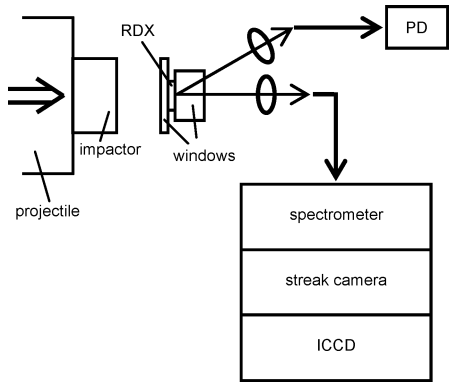

Figure 1. Experimental configuration for time-resolved emission measurements under planar shock-wave loading. The crystal is sandwiched between two optical windows. Emitted light from the shocked crystal is collected with optical fibers and detected using a diagnostic photodiode (PD) and the spectrometer/streak camera/intensified CCD detection system.

and can, therefore, be used as a sensitive signature of chemical decomposition. Hence, in the work presented here, time-resolved emission spectra were used to determine: (i) the stress threshold for decomposition, (ii) the induction time for decomposition, (iii) the stress threshold for changes in the decomposition mechanism, and (iv) the decomposition pathways.[15,19]

The specific objectives of this work were (i) to determine if shock-induced decomposition in RDX exhibits anisotropy, (ii) to quantify the anisotropy in terms of stress threshold, induction time for decomposition and the extent of decomposition, and (iii) to assess whether the shock propagation direction affects decomposition pathways.

The remainder of this paper is organized as follows. Section 2 briefly describes the experimental approach. Section 3 provides the time-resolved emission results for crystals shocked along different orientations. In sections 4 and 5 we present discussions and conclusions, respectively.

2. Experimental Approach

All the RDX single crystals used in our work were grown at the Los Alamos National Laboratory (LANL). The crystals were oriented on the (111), (210), and (100) planes and cut into thin slabs (ca. 1 mm). For shock experiments, the slabs were cleaved into smaller pieces, typically rectangular in shape, with lateral dimensions approximately 7−9 mm. Each piece was ground to a thickness of ∼400 μm and polished to an optical finish using aluminum oxide lapping sheets. The polished RDX crystals were sandwiched between two windows with a thin film of glycerol between the crystal and the windows. The front window was [100] oriented ultrapure LiF; the back window was an *a*-axis sapphire, except in the highest stress experiment which had a LiF back window. The thicknesses of the front and back windows were 3.05 and 9.5 mm, respectively.

Chemical decomposition in the shocked crystals was probed using emission spectroscopy. The experimental configuration used in this work is shown schematically in Figure 1. Because it is similar to that used in our previous work,[7,15] only a brief summary is presented here. Planar shock waves were produced by impacting the sample assembly with a 12.7 mm thick sapphire crystal mounted on a projectile that was launched using a single stage light-gas gun. Upon impact, a shock wave propagated through the front LiF window and into the RDX crystal. Because of the impedance mismatch between the windows and RDX, the sample was compressed under stepwise loading. The final stress state of the RDX crystal depends only on the impact velocity, the impactor response, and the shock wave response of the windows. Because all of these are well-known, the final stress can be determined accurately. Stress histories in the RDX crystal were calculated using a one-dimensional wave propagation code[20] and a preliminary RDX material model.[21] The final peak stresses in our experiments ranged between 7 and 20 GPa. The impact experiments are summarized in Table 1.

Light emitted from the shocked crystal was collected and delivered to the detection system using optical fibers. A tunable spectrograph with a low-dispersion grating (150 grooves/mm) provided a spectral coverage from 300 to 850 nm. The spectrally dispersed light was coupled to the streak camera/CCD detection system to record a time-dependent emission spectra. At particular times, the spectra were obtained by averaging over an appropriate number of tracks on the time axis. The spectral resolution of the system used was ∼6 nm. The time resolution, determined by the spot size on the detector, was ∼25 ns. The emission spectra were corrected for the spectral response of the detection system but not for the reabsorption effect.[7] The results of the transmission/scattering experiments indicated that the RDX crystals become "opaque" under shock wave loading, regardless of crystal orientation and, therefore, the emission is collected primarily from a thin material layer at the back of the sample.[15] However, RDX retains its crystalline form through the ring-up loading pathway, as evidenced by the Raman modes measurements.[13]

TABLE 1: Summary of Shock-Induced Emission Experiments

experiment no.	crystal orientation	crystal thickness (μm) ± 5 μm	projectile velocity (km/s) ± 0.003	peak stress (GPa) ± 0.05	total emission intensity (a.u.)
1[a]	(111)	400	0.406	7.0	0.03
2[a]	(111)	405	0.555	9.8	0.10
3	(111)	425	0.565	10.0	0.18
4[a]	(111)	330	0.646	11.5	0.61
5[a]	(111)	390	0.720	13.0	0.82
6[a,b]	(111)	390	1.606	20.0	1.00
7	(100)	422	0.566	10.0	0.62
8	(100)	445	0.571	10.0	0.79
9	(210)	410	0.409	7.0	0.06
10	(210)	425	0.565	10.0	0.74
11	(210)	422	0.566	10.0	0.72
12	(210)	390	0.720	13.0	0.90

[a] From ref 15. [b] OFHC Cu impactor and a LiF back window. Experiment performed on powder gun.

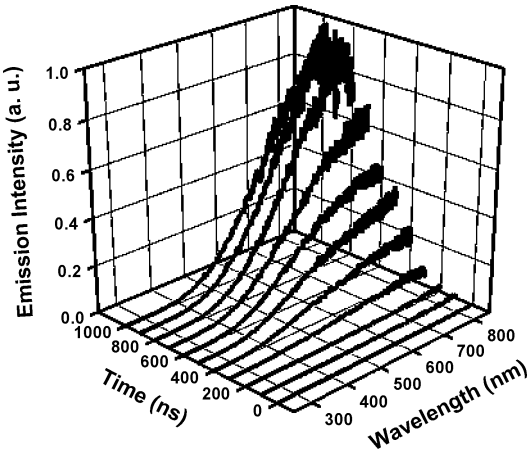

Figure 2. Time-resolved emission spectra of an RDX crystal shocked to 10 GPa, normal to the (210) plane. Spectra are corrected for the sensitivity of the detection system. The shock wave enters the crystal at 0 ns.

3. Results

3.1. General Features of Time-Resolved Emission. As presented elsewhere,[15] the observed shock-induced emission can be attributed to luminescence from species produced during RDX decomposition. Therefore, the emission intensity is related to the extent of decomposition. For this reason, we have often used the terms emission and decomposition synonymously. Typical time-resolved emission spectra of shocked RDX are shown in Figure 2. Although this result was obtained for a crystal shocked on (210), the overall features are similar to those obtained for the other two orientations. In all cases, and consistent with the previous results for the (111) orientation,[15] the observed emission starts at a specific time after the shock enters the crystal, referred to as the induction time for emission or decomposition. Furthermore, all spectra cover a broad range from 300 to 850 nm (850 nm was the long wavelength limit of our detection system). Our previous analyses indicated that the spectrum above 400 nm was associated primarily with the emission of the NO_2 radical, while below 400 nm it was associated primarily with the HONO intermediate.[15,19] Emission spectra for crystals shocked to 10 GPa along the three different orientations are compared at selected times in Figure 3. The temporal evolution observed for the three orientations is similar: the long wavelength contribution to the spectra increases with time. However, detailed comparisons of the spectra indicate noticeable differences among the crystal orientations with respect to emission intensity and time evolution of the spectral shape.

3.2. Emission Intensity (Decomposition Extent). ***A. Time Dependence.*** Figure 4 shows the temporal evolution of the emission intensity, integrated over the range of wavelengths from 300 to 850 nm, along with the calculated stress history in the middle of the sample. Results are presented for crystals shocked on the (210), (100), and (111) planes to the same peak stress of 10 GPa. Distinct differences are observed in both the onset and intensity of emission. The (111) orientation clearly shows the longest induction time for emission and the lowest emission intensity. Note that the measured induction time and emission intensity are the result of the combination of the loading path and chemical kinetics. One should also notice that the emission starts before the uniform final stress is reached in the sample. However, because the loading paths are similar for three orientations, the observed differences in emission profiles reflect differences in the decomposition processes. We point

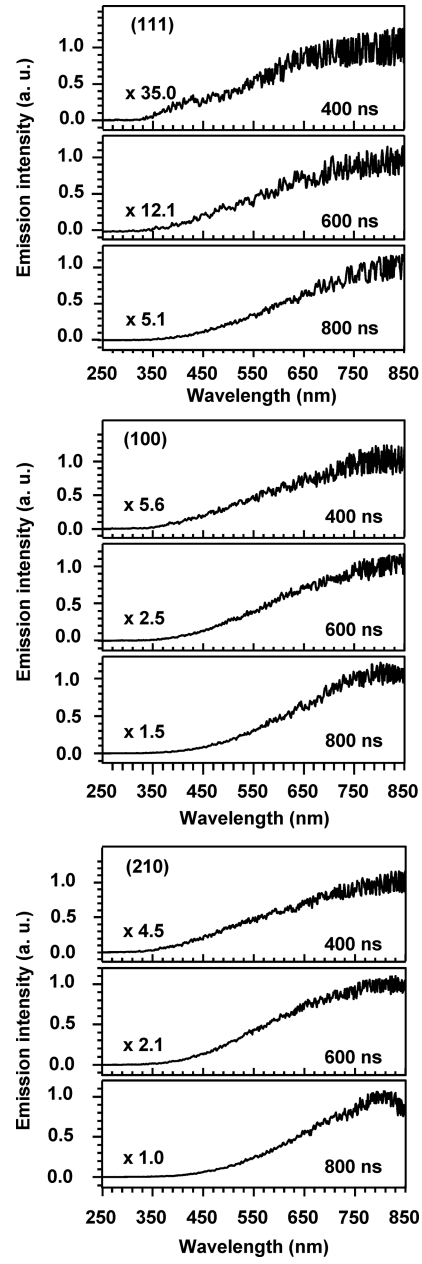

Figure 3. Selected time-resolved emission spectra of RDX crystals shocked to 10 GPa, normal to the (111), (100), and (210) planes to 10 GPa. In all cases, the emission intensity is related to the intensity obtained at 800 ns for the crystal shocked normal to the (210) plane. The shock wave enters the crystal at 0 ns.

out that the data for the (111) and (210) orientations were quite reproducible but the data for the (100) orientation showed some variation. The latter is consistent with the observations in the wave profiles of the (100) oriented crystals.[22] Because of this difficulty, we were unable to determine definitively whether the (210) or the (100) orientation exhibited the greater emission intensity. Nevertheless, both orientations demonstrated much stronger emission than the (111) orientation. This implies that decomposition in crystals shocked on the (210) and (100) planes proceeds at higher rates than crystals shocked on the (111) plane. A quantitative comparison of emission intensities and induction times for the three orientations can be found in Tables 1 and 2. These results reveal that at 10 GPa, the (111) orientation is less sensitive to shock initiation than the (210) and (100) orientations.

B. Stress Dependence. Figure 5 shows temporal profiles of the spectrally integrated emission intensity, normalized to the

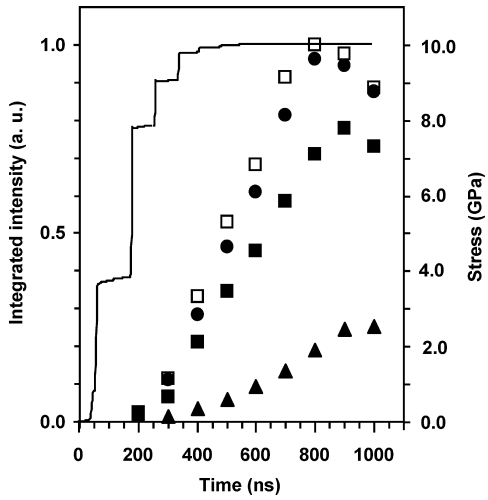

Figure 4. Spectrally integrated emission intensity as a function of time for RDX crystals shocked to 10 GPa, normal to different orientations: (▲) (111), experiment 3; (■) (100), experiment 7; (□) (100), experiment 8; (●) (210), experiment 10. Solid line represents the calculated stress history at mid point of the RDX crystal. The shock wave enters the crystal at 0 ns.

TABLE 2: Induction Time (±25 ns) to Emission for RDX Crystals Shocked along Different Orientations to Different Peak Stresses

	orientation		
stress (GPa)	(210)	(100)	(111)
7	300		445[a]
10	125	125	345
13	75		275[a]
20			45[a]

[a] Data obtained from ref 15.

maximum value in each case, for crystals shocked to peak stresses of 7, 10, and 13 GPa. We compare the (210) and (111) oriented crystals because they exhibited the strongest and the weakest emission intensities, respectively. At all stresses, both the induction times and the emission rise times are shorter for crystals shocked on the (210) plane than on the (111) plane (see Table 2 for values of induction times). Also, the results in Figure 5 demonstrate that both the induction time and the emission rise time decrease with increasing stress.

In Figure 6, we show the stress dependence of the total emission intensity, the intensity integrated over the wavelengths and time. The lines in the graph are smooth fits and serve only to guide the eye. At all stresses, the total emission intensity is larger for shocks on the (210) plane than on the (111) plane. The stress threshold for emission has not been determined precisely but appears to be around 5 GPa; it is lower for the (210) orientation than for the (111) orientation The total emission intensities appear S-shaped with respect to stress; the difference in intensities between two orientations changes nonmonotonically with stress. The stress threshold for emission acceleration is lower for the (210) orientation (est. ~8 GPa) than for the (111) orientation (est. ~10 GPa). The total emission intensity at higher stresses tends to a similar value for both orientations. Collectively, these features indicate the anisotropic nature of RDX decomposition and reveal increased sensitivity in crystals shocked on the (210) plane than on the (111) plane.

3.3. Emission Spectra Shape (Decomposition Intermediates). ***A. Time Dependence.*** Just as spectral features are signatures of specific chemical species, changes observed in spectral features with time are signatures of changing decomposition pathways.[15,19] To determine the anisotropy in decomposition pathways, we examined changes in the emission spectra shapes for the three orientations. Figure 7 presents emission spectra for crystals shocked on the (210), (100), and (111) planes to the same peak stress (10 GPa). To facilitate comparison, we normalized the emission spectra for different orientations to the same maximum value and compared the spectra obtained at 400 and 800 ns after the shock entered the crystal. These two times correspond to initial and later stages of decomposition. The spectra are quite similar early on (panel A in Figure 7), indicating comparable contributions of the emitting species to the spectra for the three orientations during the early stages of decomposition. The emission spectra evolve differently with time. The contributions of the emission intensities at long wavelengths (LW, above 650 nm) relative to the total emission

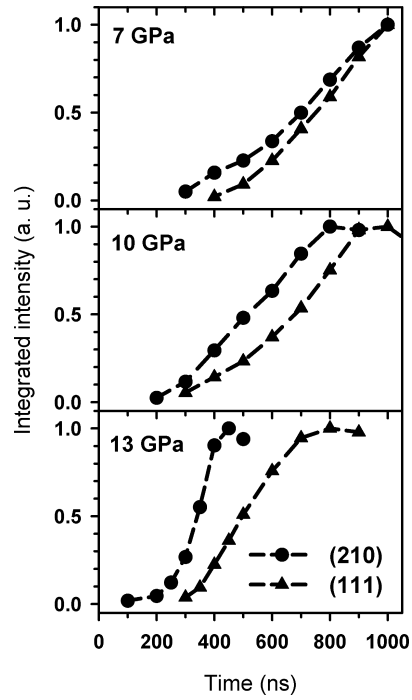

Figure 5. Spectrally integrated emission intensity as a function of time for RDX crystals shocked to different stresses, normal to two planes: (●) (210) and (▲) (111). The shock wave enters the crystal at 0 ns. Dashed lines are a guide to the eye.

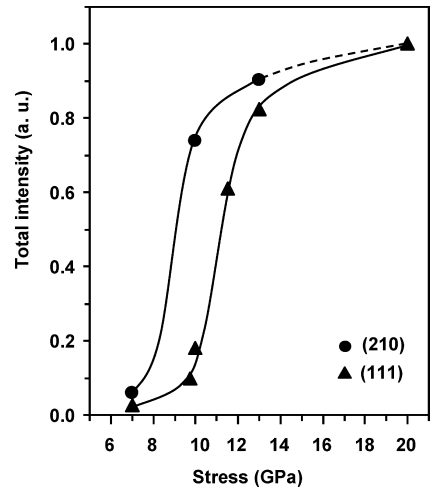

Figure 6. Stress dependence of total emission intensity for RDX crystals shocked normal to two planes: (●) (210) and (▲) (111). Lines are drawn to guide the eye.

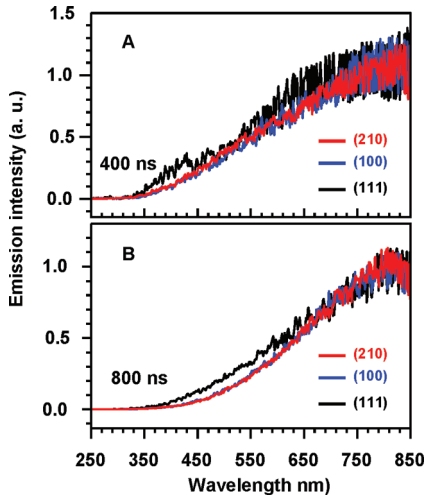

Figure 7. Emission spectra for RDX crystals shocked to 10 GPa, normal to different planes: (111), black line; (100), blue line; (210), red line. The spectra shown in panels A and B are obtained at 400 and 800 ns, respectively, after the shock entered the crystal. Irregularity in a curve shape around 400 nm (panel A, 400 ns) for (111) orientation is likely caused by noise. The maximum intensity for each spectrum is normalized to the same value.

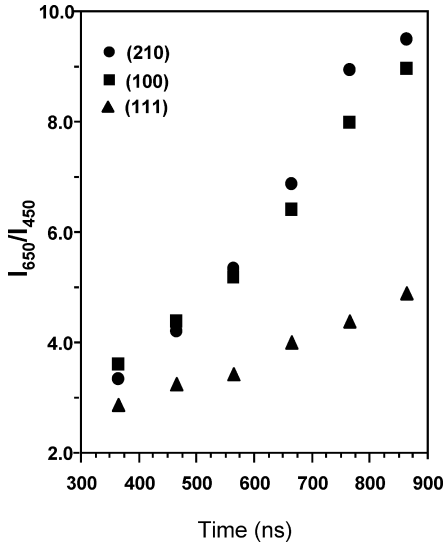

Figure 8. Ratio of emission intensity at 650 nm to that at 450 nm as a function of time for RDX crystals shocked to 10 GPa, normal to different planes: (▲) (111), experiment 3; (■) (100), experiment 5; (●) (210), experiment 8.

intensities are larger for the (210) and (100) orientations than for the (111) orientation.

To quantify spectra shape changes, we compared intensity ratios at 650 nm (LW) and at 450 nm, I_{650}/I_{450}, as a function of time. Although these wavelengths are somewhat arbitrary, they permit consistent comparisons of different conditions.[15] The ratios are plotted in Figure 8 for crystals shocked along the three orientations to a final stress of 10 GPa. At early times, the ratios are comparable for the three orientations, indicating comparable contributions of emitting species to the short and long wavelength spectra. At later times, the long wavelength contributions to the spectra increase and the increase is much larger for the (210) and (100) orientations than for the (111) orientation. Because the shapes of the emission spectra are linked to the decomposition pathways,[15] it implies that the relative contribution of the decomposition pathways to emission is orientation dependent. Below we examine this inference by comparing results at different stresses.

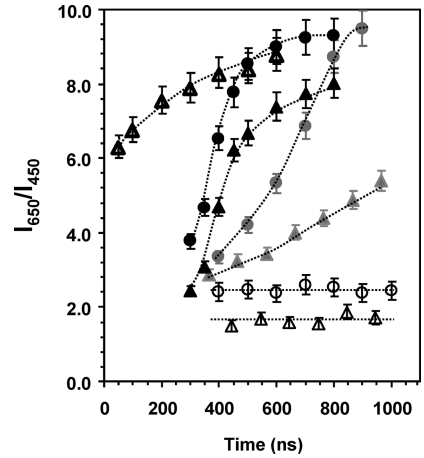

Figure 9. Ratio of emission intensity at 650 nm to that at 450 nm as a function of time for RDX crystals shocked normal to (111) (triangles) and (210) (circles) planes to different stresses: 7 GPa (open symbols), 10 GPa (gray symbols), 13 GPa (solid symbols), and 20 GPa (bold symbol).

B. Stress Dependence. Figure 9 presents a comparison of the ratio of emission intensity at 650 nm to intensity at 450 nm as a function of time for crystals shocked to different peak stresses on the (210) and (111) planes. The data cutoff times vary, depending on the time the release waves entered the crystal. Below 7 GPa, the spectral shape for both the (210) and (111) oriented crystals remains flat. However, the ratio is higher for the (210) orientation than for the (111) orientation. Above 7 GPa, the I_{650}/I_{450} ratio increases with time; that is, the LW component (part of spectrum above 650 nm) becomes dominant in the spectrum. At selected stresses and fixed times, the LW component makes a consistently larger contribution to the spectra for shocks on the (210) plane than on the (111) plane. As peak stress rises, the spectral profile of the emission changes, with the LW component dominating the emission spectrum. The time required for the spectral change to occur decreases with increasing stress, and for both orientations, the spectral shape of emission tends to the same steady shape at later times and higher stresses. This suggests that the same decomposition pathways, as previously proposed for the (111) orientation [15, 19], are likely operative for crystals shocked along different orientations.

4. Discussion

The light emission results suggest that RDX crystals exhibit anisotropic shock-induced decomposition response. This is manifested in the stress threshold for decomposition, in the stress threshold to accelerate decomposition, in the induction time to decomposition, and in the extent of decomposition. Our studies for three crystal orientations provide strong evidence that RDX is less sensitive to decomposition when shocked on the (111) plane and more sensitive when shocked on the (210) or (100) planes.

Although the shock sensitivity of energetic crystals results from complex coupling between mechanical, thermal, and chemical effects, the work on shocked PETN crystals demonstrated a link between mechanical response and shock-induced chemical decomposition. Therefore, to understand our emission/decomposition results, it is useful to relate these results to the mechanical anisotropy of shocked RDX. Under shock wave loading conditions, inelastic deformation in molecular crystals often occurs through dislocation motion on preferred slip systems. As inferred from the work on PETN, one might expect

that the shock loading along more sensitive orientations will encounter more hindrance to shear deformation compared to shock loading along the less sensitive orientations. However, initiation in PETN occurs at stresses just above dynamic yielding in some orientations. RDX initiation occurs at appreciably higher stresses, where phase behavior and stress- and rate-induced changes in dissipative mechanisms may cause increased difficulty in developing a molecular interpretation of continuum observations.

Emission/decomposition was observed from RDX crystals shocked to peak stresses of at least 7 GPa; there was no detectable emission below stresses of 5 GPa. As shown previously, RDX crystals shocked to stresses higher than 4.5 GPa undergo a structural phase transition ($\alpha-\gamma$).[13] Thus, the observed emission likely takes place when the crystal is in the high pressure γ-phase. The effect of the phase transition on the response of RDX to shock-induced decomposition may significantly change the response from what might be predicted on the basis of the ambient α-phase response. However, the emitting γ-phase is a result of unixial loading of a specific orientation of the α-phase, so it is useful to examine the pathway to the ultimate state of reaction even if the specific pathway and structure is not known. In addition, in the stepwise loading process, the initial stresses imposed on the crystal for experiments to final stresses of 10 GPa or less were below the phase transition stress. To account for the observed anisotropic sensitivity, the anisotropy in the mechanical response of RDX in the low pressure phase (α-RDX) needs to be considered. Two factors might contribute to the anisotropic response: activation of slip systems known from the quasistatic experiments, and activation of new slip systems under shock-wave loading. Below, we briefly discuss the potential contributions of these factors to the observed anisotropy to decomposition.

RDX crystals impacted on (111), (210), or (100) planes provide access to 6, 5, and 0 known slip systems,[16,17] respectively. These slip (or shear) planes are shown in Figure 10, where the shear planes are viewed edge-on and shear displacement comes out of the page toward the viewer. The difference between the (111) and (210) orientations is that (111) shocks activate the (010)[001] slip system, whereas (210) shocks do not. Therefore, the difference in the shock response of two orientations can be discussed in terms of the (010)[001] slip system. To assess whether this slip system differs from other remaining systems, we compared the resolved shear stresses (RSS) and degree of steric hindrance for the known slip planes. The calculated value of RSS for the (010)[001] slip system is not significantly different from the values for the other slip planes.[21] However, inspection of Figure 10 suggests that the (010)[001] slip system is somewhat less hindered compared to slip having shear displacements in the [100] direction. Since the (010)[001] slip system cannot be activated by shocks normal to the (210) plane, from these crystallographic considerations one would expect lower sensitivity to decomposition for shocks on the (111) plane and a larger sensitivity for the (210) plane. Our emission results for (111) and (210) orientations are consistent with these expectations.

However, recent large-scale molecular dynamics (MD) simulations of the shock propagation in oriented RDX single crystals indicated that additional slip systems can be activated under shock loading, which are not observed under quasistatic conditions.[11] In particular, the simulations predict that, for stresses larger than 1.3 GPa, shock waves on the (111) plane can activate the (001)[010] slip system. For this slip system, activation is predicted to occur by homogeneous nucleation of

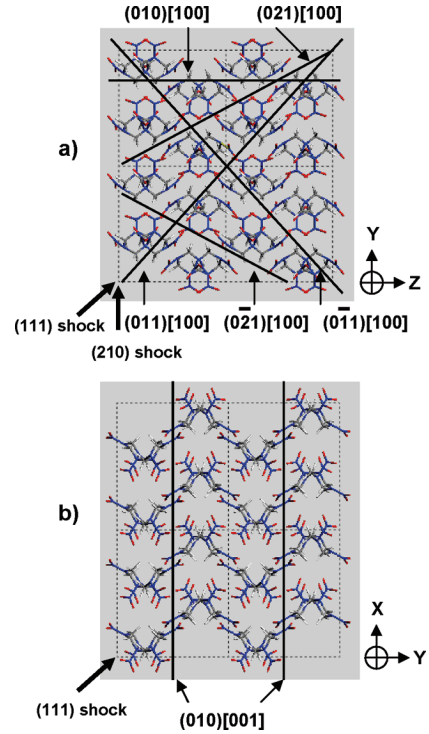

Figure 10. Views of RDX crystal structure at ambient conditions. Eight cells are shown. The following atoms are in molecules: oxygen (red), nitrogen (blue), carbon (gray), and hydrogen (white). Shears occur along the slip plane in a direction toward the viewer. (a) View of shear planes for the (111) and (210) shocks. (b) View of shear plane for the (111) shock.

partial dislocation loops that in turn can form a high density of stacking faults in the shock-compressed crystal. It was proposed that these stacking faults would harden the crystal by forming a barrier for the glide of perfect dislocations on other slip systems. Because of this anomalous plastic hardening, it was proposed that (111) oriented RDX would be more sensitive to initiation than (210). However, this prediction is not supported by the results of our emission experiments. There is insufficient information to conclude that the anomalous plastic hardening observed in the previous simulations does not result in an increase in crystal sensitivity under shock loading; the simulations were for weak shocks in the α-phase, while the experiments are relatively stronger shocks in the γ-phase. Further, it is not known if the ring-up process affects activation of the predicted hardening mechanism. Single-shock measurements of reaction initiation in oriented RDX crystals, similar to the previous work on PETN, would help address this issue.

Regarding shocks on the (100) plane, our experiments indicate that the emission intensity for this orientation is comparable to the emission intensity for the (210) orientation. Since the shocks on the (100) plane have access to no known slip systems, shear stresses may not be relieved readily through a slipping mechanism. Therefore, the sensitivity of the (100) oriented crystal may be governed by other factors. Indeed, work by Hooks et al.[22] pointed out the possible consequences of intrinsic microcracks and voids on the mechanical response of the (100) oriented crystals. Furthermore, MD simulations by Cawkwell et al.[23] suggested nucleation and growth of shear bands at 9.7 GPa for RDX crystal shocked on the (100) plane. The formation of these shear bands was related to intrinsic instabilities in the crystal structure. Together, these findings suggest that the

sensitivity to decomposition for the (100) oriented crystals cannot be explained simply using the concept of shearing along slip planes.

The brief discussion presented above suggests that the relation between chemical decomposition and mechanical response for RDX crystals may be more complex than that observed for PETN crystals. For example, on one hand, the low sensitivity to decomposition of the (111) oriented crystal seems to be consistent with the concept of steric hindrance to shear deformation. However, the low sensitivity of the (111) oriented crystal appears to contradict expectations based on the anomalous plastic hardening observed under shock loading in MD calculations, although there are differences in shock strength, loading path, and phase. To address these issues, better understanding of the mechanical response of RDX crystals under stresses relevant to our experiments is needed to properly account for the observed differences in the anisotropy to decomposition.

5. Conclusions

We have demonstrated that many aspects of shock-induced decomposition in RDX crystals display significant anisotropy. Decomposition was probed using time-resolved emission spectroscopy to capture differences in crystals shocked on the (210), (111), and (100) planes to peak stresses between 7 and 20 GPa. Clear differences in the induction time to decomposition, extent of decomposition, and spectral distribution of decomposition species with stress and time were observed for the three orientations. These results reveal that the (210) and (100) orientations are more sensitive to shock initiation than (111) oriented crystals. The differences in sensitivity between these three crystal orientations are not well understood on the basis of the current knowledge of the anisotropic mechanical properties of RDX crystals. The relation between mechanical response and chemical initiation for RDX may be more complex than that observed for PETN crystals.

Finally, our emission results clearly demonstrate that spectra shapes evolve with time and stress differently for different orientations. The observed differences are rather quantitative than qualitative; regardless of the crystal orientation, the spectra are composed of the same three components and cover the same spectral range at all stresses and times. The difference between these three orientations is such that the spectral shapes for the (111) orientation follow the spectral shapes for two other orientations with a delay in time and stress. With increasing time and stress, all spectra tend to have similar shapes dominated by the long wavelength component. Because the emission spectra are related to the decomposition processes in shocked crystals, these observations indicate that similar decomposition pathways are likely operative for all three orientations.

Acknowledgment. We thank Dr. J. M. Winey for useful discussions and for helpful comments regarding the manuscript. K. Zimmerman, K. Perkins, and C. Bakeman are thanked for their assistance in performing the shock experiments. This work was supported by ONR MURI Grant N00014-06-1-0459 and DOE Grant DEFG0397SF21388.

References and Notes

(1) Dick, J. J. *Appl. Phys. Lett.* **1984**, *44*, 859.
(2) Dick, J. J.; Mulford, R. N.; Spencer, W. J.; Pettit, D. R.; Garcia, E.; Shaw, D. C. *J. Appl. Phys.* **1991**, *70*, 3572.
(3) Dick, J. J.; Ritchie, J. P. *J. Appl. Phys.* **1994**, *76*, 2726.
(4) Dick, J. J. *J. Appl. Phys.* **1997**, *81*, 601.
(5) Winey, J. M.; Gupta, Y. M. *J. Appl. Phys.* **2010**, *107*, 103505.
(6) Gruzdkov, Y. A.; Gupta, Y. M. *J. Phys. Chem. A* **2000**, *104*, 11169.
(7) Dreger, Z. A.; Gruzdkov, Y. A.; Gupta, Y. M.; Dick, J. J. *J. Phys. Chem. B* **2002**, *106*, 247.
(8) Gruzdkov, Y. A.; Dreger, Z. A.; Gupta, Y. M. *J. Phys. Chem. A* **2004**, *108*, 6216.
(9) Hemmi, N.; Dreger, Z. A.; Gruzdkov, Y. A.; Winey, J. M.; Gupta, Y. M. *J. Phys. Chem. B* **2006**, *110*, 20948.
(10) Hooks, D. E.; Ramos, K. J.; Martinez, A. R. *J. Appl. Phys.* **2006**, *100*, 024908.
(11) Cawkwell, M. J.; Ramos, K. J.; Hooks, D. E.; Sewell, T. D. *J. Appl. Phys.* **2010**, *107*, 063512.
(12) Dreger, Z. A.; Gupta, Y. M. *J. Phys. Chem. B* **2007**, *111*, 3893.
(13) Patterson, J. E.; Dreger, Z. A.; Gupta, Y. M. *J. Phys. Chem. B* **2007**, *111*, 10897.
(14) Dreger, Z. A.; Patterson, J. E.; Gupta, Y. M. *J. Phys.: Conf. Ser.* **2008**, *121*, 042012.
(15) Patterson, J. E.; Dreger, Z. A.; Miao, M. S.; Gupta, Y. M. *J. Phys. Chem. A* **2008**, *112*, 7374.
(16) Gallagher, H. G.; Halfpenny, P. J.; Miller, J. C.; Sherwood, J. N. *Philos. Trans. R. Soc. London, Ser. A* **1992**, *339*, 293.
(17) Ramos, K. J.; Hooks, D. E.; Bahr, D. F. *Philos. Mag.* **2009**, *89*, 2381.
(18) Choi, C. S.; Prince, E. *Acta Crystallogr. B* **1972**, *28*, 2857.
(19) Miao, M. S.; Dreger, Z. A.; Patterson, J. E.; Gupta, Y. M. *J. Phys. Chem. A* **2008**, *112*, 7383.
(20) Gupta, Y. M. *COPS code*; Stanford Research Institute: Menlo Park, CA, U.S., 1976, unpublished.
(21) Winey, J. M. Personal communication.
(22) Hooks, D. E.; Ramos, K. J.; Bahr, D. F. In *Shock Compression of Condensed Matter*; Elert, M., Furnish, M. D., Chau, R., Holmes, N., Nguyen, J., Eds.; AIP: Melville, NY, U.S., 2007; p 789.
(23) Cawkwell, M. J.; Sewell, T. D.; Zheng, L.; Thompson, D. L. *Phys. Rev. B* **2008**, *78*, 014107.

JP106892C